Electronic Supplementary Information

Crystallization driven boost in fill factor and stability in additive-free organic solar cells

David Garcia Romero, Lorenzo di Mario, Giuseppe Portale and Maria Antonietta Loi*

Zernike Institute for Advanced Materials University of Groningen

Nijenborgh 4, Groningen 9747 AG, The Netherlands.

*E-mail: m.a.loi@rug.nl

1. Absorption

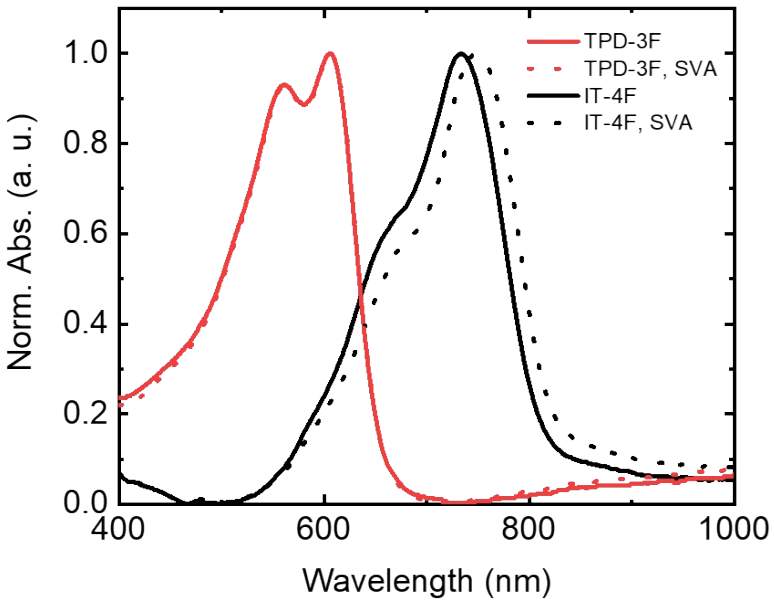

Figure S1. Absorbance of neat acceptor and neat donor films with and without SVA.

2. Additive-free OSCs chart

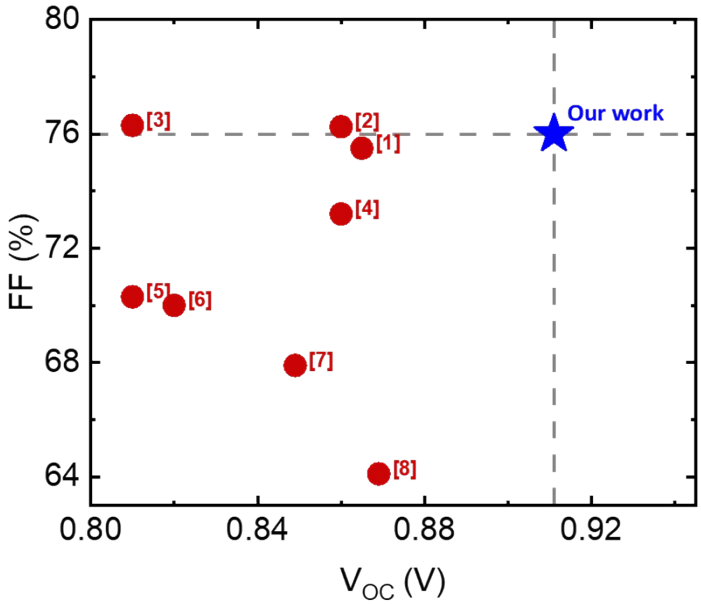

Figure S2. Scatter plot of reported high efficiency (>13% PCE) additive-free OSCs. [1–8]

3. Air stability

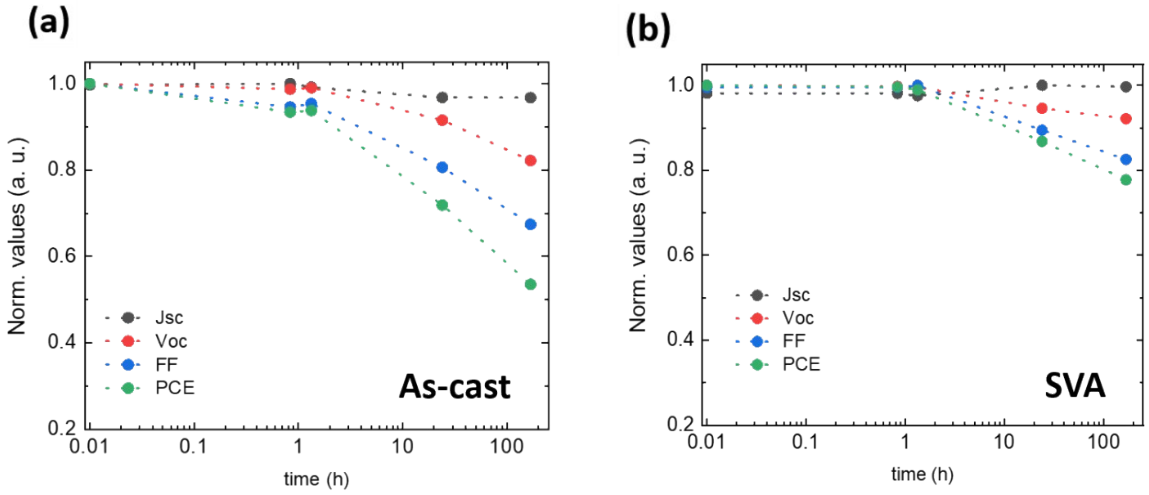

Figure S3. Stability test in ambient conditions (T = 21°C, RH = 45%)

4. Morphology

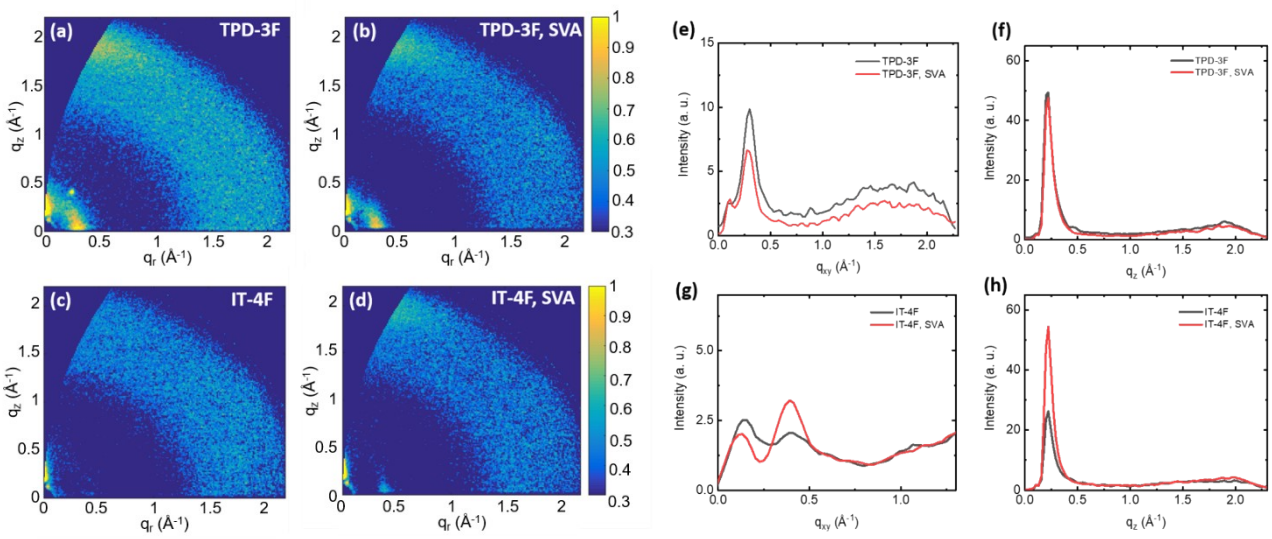

Figure S4. 2-D GIWAXS images for neat TPD-3F **(a,b)** and IT-4F **(c,d)** films with and without solvent vapor annealing and the corresponding in-plane **(e,g)** and out-of-plane **(f,h)** cuts.

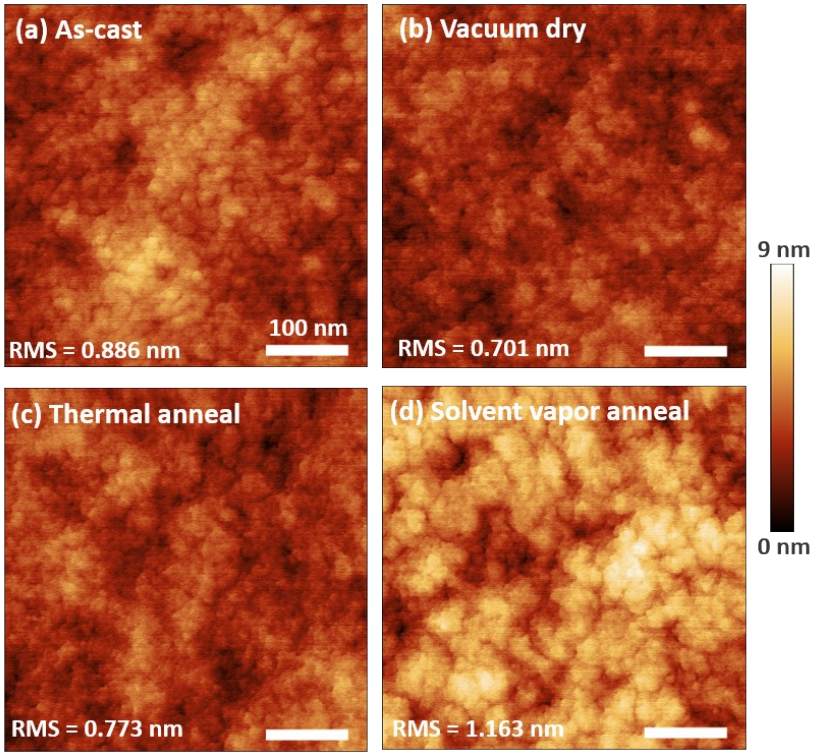

Figure S5. Surface topographic AFM images of the active layer deposited on glass/ITO/PEDOT:PSS substrate for the four different conditions.

5. Light dependence

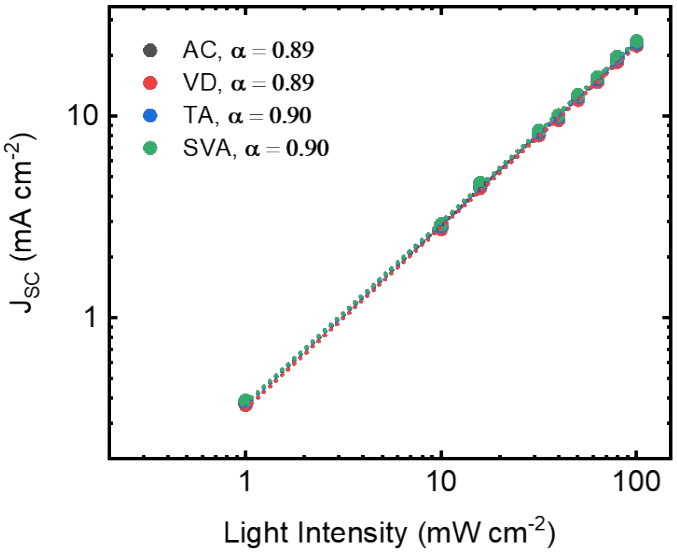

Figure S6. J_{SC} vs light intensity.

Table S1. Mott-Schottky relation extracted parameters.

Post-treatment	V_{BI} (V)	N_A (cm^{-3})	ϵ_r
As-cast	1.05	1.21×10^{16}	3.85
Vacuum drying	1.03	1.19×10^{16}	3.96
Thermal anneal.	1.03	1.22×10^{16}	3.84
Solvent vapor anneal.	0.91	1.09×10^{16}	3.54

6. Photoluminescence

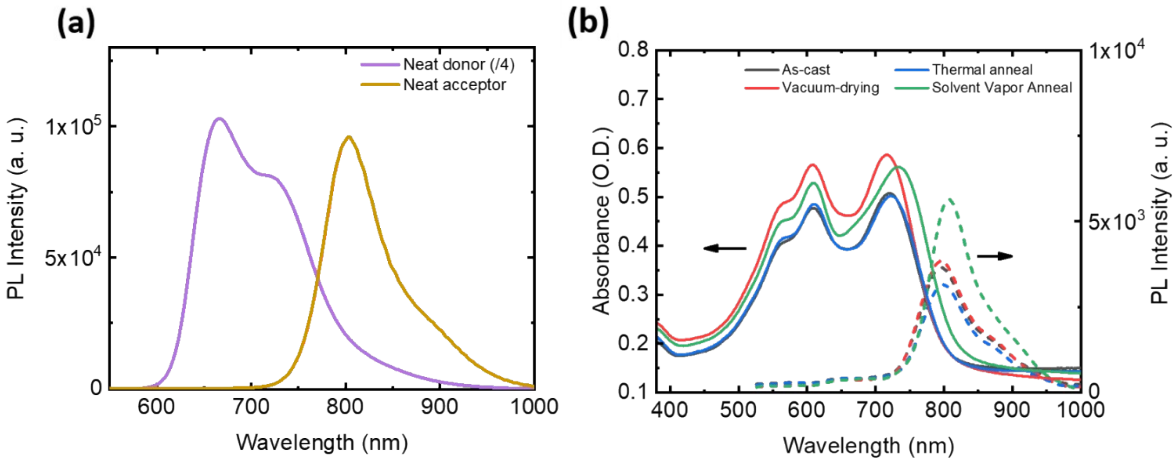

Figure S7. Steady-state PL of neat materials **(a)** and absorbance and PL of the blends **(b)**

Table S2. Calculated lifetimes from the time-resolved PL decays.

Post-treatment	<τ> (ps)
As-cast	21.30
Vacuum drying	22.98
Thermal anneal.	18.33
Solvent vapor anneal.	17.04

References

1. Liu Q, Jiang Y, Jin K, Qin J, Xu J, Li W, et al. 18% Efficiency organic solar cells, *Science Bulletin*, 2020, **65**, 272–5.

2. Zhou Z, Liu W, Zhou G, Zhang M, Qian D, Zhang J, et al. Subtle Molecular Tailoring Induces Significant Morphology Optimization Enabling over 16% Efficiency Organic Solar Cells with Efficient Charge Generation, *Advanced Materials*, 2020, **32**, 1906324.

3. Xu X, Feng K, Bi Z, Ma W, Zhang G, Peng Q. Single-Junction Polymer Solar Cells with 16.35% Efficiency Enabled by a Platinum(II) Complexation Strategy. *Advanced Materials*, 2019, **31**, 1901872.

4. Yuan J, Zhang Y, Zhou L, Zhang G, Yip HL, Lau TK, et al. Single-Junction Organic Solar Cell with over 15% Efficiency Using Fused-Ring Acceptor with Electron-Deficient Core, **Joule**, 2019, **3**, 1140–51.

5. Zhao H, Naveed HB, Lin B, Zhou X, Yuan J, Zhou K, et al. Hot Hydrocarbon-Solvent Slot-Die Coating Enables High-Efficiency Organic Solar Cells with Temperature-Dependent Aggregation Behavior, *Advanced Materials*, 2020, **32**, 2002302.

6. Guo Q, Lin J, Liu H, Dong X, Guo X, Ye L, et al. Asymmetrically noncovalently fused-ring acceptor for high-efficiency organic solar cells with reduced voltage loss and excellent thermal stability, *Nano Energy*, 2020, **74**, 104861.

7. Wang W, Zhao B, Cong Z, Xie Y, Wu H, Liang Q, et al. Nonfullerene Polymer Solar Cells Based on a Main-Chain Twisted Low-Bandgap Acceptor with Power Conversion Efficiency of 13.2%, *ACS Energy Letters,* 2018, **3**, 1499–507.

8. Cui Y, Yao H, Zhang J, Zhang T, Wang Y, Hong L, et al. Over 16% efficiency organic photovoltaic cells enabled by a chlorinated acceptor with increased open-circuit voltages, *Nature Communications*, 2019, **10**, 2515.